2-D Magnetotellurics and Gravity at the Geothermal Site at Soultz-sous-Forêts

Eva Schill[1,2], Johannes Geiermann[2] and Jessica Kümmritz[2]

[1]Laboratoire de Géothermie, Université de Neuchâtel, Switzerland

[2]Institut für Geothermisches Ressourcenmanagment, ITB gGmbH, Bingen, Germany

eva.schill@unine.ch

Keywords: 2-D magnetotellurics, gravity, Soultz-sous-Forêts, geophysical exploration

ABSTRACT

With the aim of investigating the possibilities of magnetotelluric methods and gravity for exploration of potential EGS sites in the Upper Rhine valley, a 2-D magnetotelluric and 3-D inversion of existing gravity data on the basis of a 3-D geological model have been carried out in the area of the geothermal power plant of Soultz-sous-Forêts. A magnetotelluric survey was executed on a 12 km long profile across the thermal anomaly in the winter 2007/08. Despite strong artificial noise, processing using remote referencing and Sutarno phase consistent smoothing revealed significant results from 10 out of 16 sites. Indication for 1-D structures were found in the shortest periods, 2-D effects in the periods <40 s, and 3-D effects in the long period range. Since 3-D effects were found in the longer periods, 2-D inversion was carried to periods <40 s. The results of the 2-D MT inversion are consistent with the geology of the geothermal site and distinguish well the sediments from the granitic basement including the structures given by the faults. A conductive anomaly with a resistivity of about 3 Ω m has been found at a depth down to 2000 m in the area of the Soultz- and Kutzenhausen faults, which is attributed to circulation of geothermal brine. A corresponding density anomaly has been observed in the 3-D inversion of existing gravity data in combination with a 3-D geological model. In the area of the two major faults, a decrease of the mean density in the granitic basement of about 250 kg/m^3 to 2500 kg/m^3 has been attributed to an increase in porosity. A second density anomaly has been found to the North of the geothermal reservoir. In this case, an increase of the mean density has been observed, which indicates an inhomogeneity in the basement.

1. INTRODUCTION

The Upper Rhine valley reveals favorable condition for exploitation of geothermal energy. This is supported by different local heat flow anomalies with a maximum of 140 mW m^{-2} at the geothermal site of Soultz-sous-Forêts (Schellschmidt and Clauser, 1996) and temperature anomalies at depth (Hurter and Schellschmidt, 2003). Local heat flow and temperature maxima in the Upper Rhine valley originate from a strong convectional heat transport mainly in the granitic basement (Bächler, 2003). Such systems may be exploited using Enchanced Geothermal System (EGS) technology. By definition these systems are characterized by appropriate temperature at depth and natural permeability, which is improved by stimulation techniques. The challenge of geothermal prospection is to predict temperature, permeability and stress orientation in the subsurface. In the case of the Soultz reservoir, besides the heat flow anomaly, temperature condition with a local geothermal gradient of 100 K km^{-1} was known prior to the first geothermal well: Furthermore, the orientation of faults was known from the sedimentary cover (Genter, 1989). Yet further information were gained after drilling GPK1 and deepening of the EPS1 well to approximately 2000 m and later drilling GPK 2-4 to 5000 m. Here should be mentioned, the investigation of a porosity of <3 % in the unaltered granite and about 8% in the reservoir granite using neutron porosity hydrogen index (Genter, 1989), the hydraulic conductivity (6.6 10^{-8} to 2.3 10^{-6} m s^{-1}) evaluating tracer tests (Aquilina *et al.*, 2003) and the fracture orientation (Genter, 1989, Dezayes and Genter, 2008), which reveals a major change in orientation of the stress field between the sedimentary cover and the granitic basement. On the basis of the vertical temperature distribution of the 5000 m wells, the natural permeability of about up to 3·10^{-14} m^2 was inferred (Kohl *et al.*, 2000).

The wide range of density in sedimentary rocks is primarily due to variations in porosity. Although igneous rocks generally are denser than sedimentary rocks, strong fracturation may contribute to a significant reduction in density (Telford *et al.*, 1990). In the past, investigation of gravity in the Upper Rhine graben aimed the understanding of the deep structure of the graben, such as the shallow MOHO (Gutscher, 1995) and the internal structure of the graben (Rotstein *et al.*, 2006). A detailed study on the gravity in the area of the geothermal site of Soultz-sous-Forêts in combination with magnetic analysis revealed Variscian tectonic inheritance (Edel *et al.*, 2007).

Since magnetotellurics is an electromagnetic method, it is primarily used to detect conductivity differences in the subsurface. It is in the nature of induction based methods that they may provide significant response from structures of high electric conductivity (Simpson and Bahr, 2005). Geothermal brine in the Upper Rhine graben reveals considerable high salinity of about 100 g l^{-1} at the Soultz site (Pauwels *et al.*, 1992), which results in high mean electric conductivities in the range of about 10 Si m^{-1} at reservoir temperature of about 200 °C. Furthermore, electric conductivity itself is a temperature dependent parameter, which may be of use for geothermal prospection (Spichak *et al.*, 2007). The relation between effective porosity and electric conductivity described by Archie's law (Archie, 1942) may also lead to further indication on porosity changes in the subsurface.

First 1D magnetotelluric studies performed in the vicinity of GPK1 at the Soultz geothermal site (Marquis and Gilbert, 2002) have indicated the possibility of detection of geothermal brine at Soultz. Two positive conductivity anomalies were interpreted as the "Couche rouge" layer at a depth of approximately 500 m and a brine bearing fault at approximately 1500 m depth, which is in agreement with the results from 2-D seismic interpretation. Earlier electromagnetic studies refer to the Rhine graben as conductive regional structure (Teufel, 1986; Tezkan, 1994; Babour and Mossier, 1980; Albouy and Fabriol, 1981).
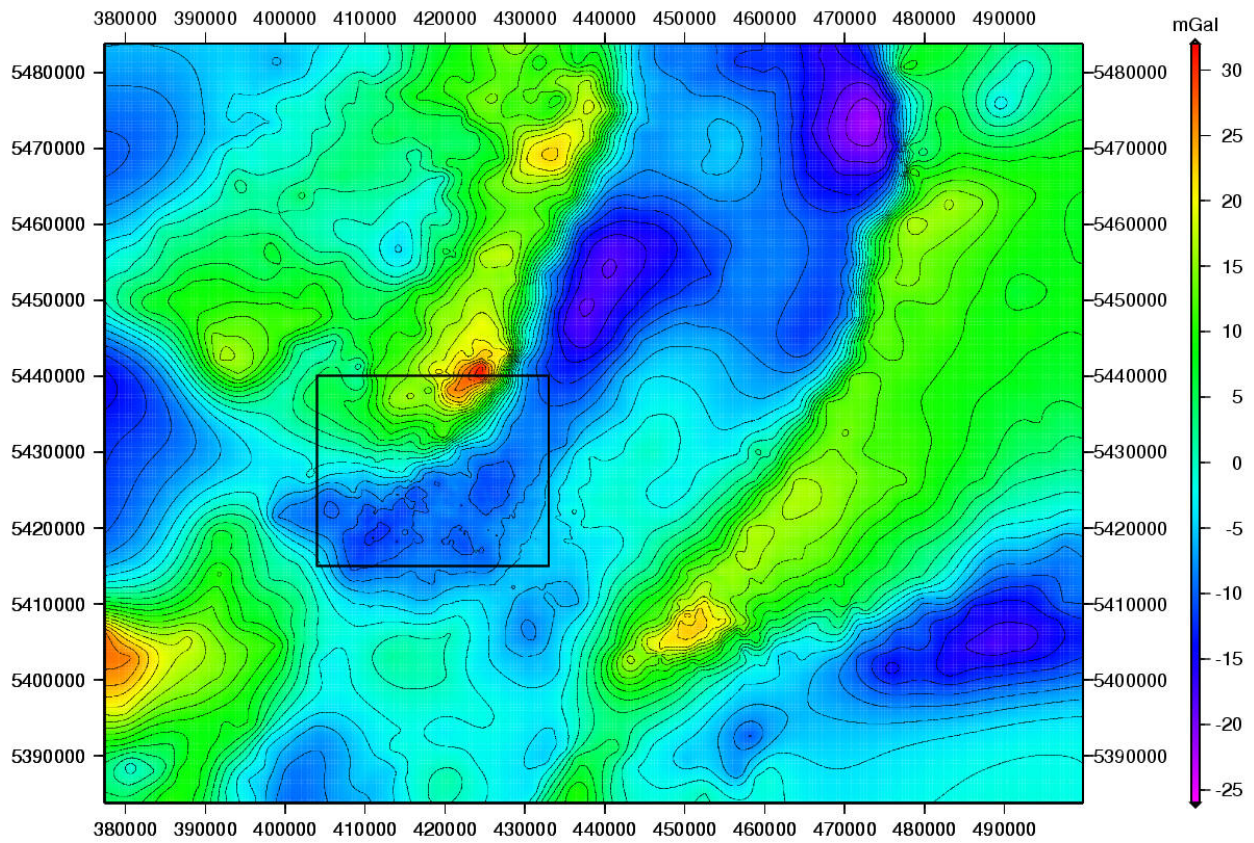
Figure 1: Residual Bouguer anomaly of the area of the geothermal site at Soultz-sous-Forêts (black rectangle) and the larger area of investigation for boundary effects.
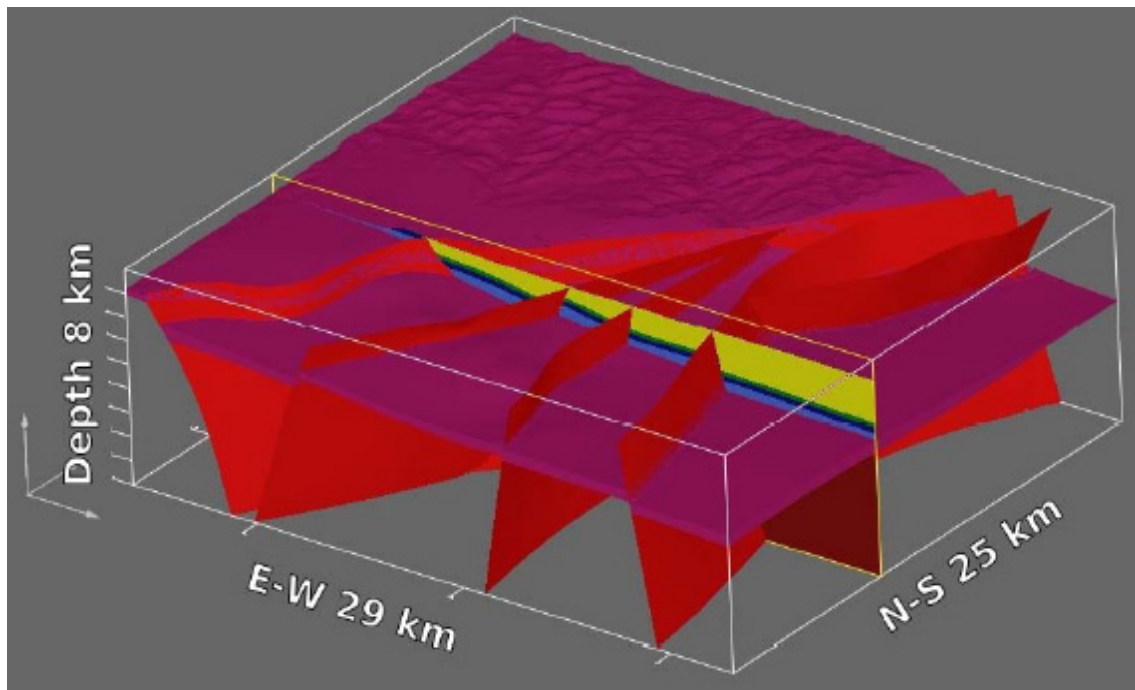

Figure 2: Regional geological 3D model of the geothermal area of Soultz-sous-Forêts including the formations Tertiary, Jurassic, Keuper, Muschelkalk, Buntsandstein and granitic basement (from top to bottom) and the Main Boundary Fault, the Soultz- Kutznhauesen- and Reimerswiler Faults (Schill *et al.*, 2009).

Some of these studies focus on the deep structure of the Rhine graben using long periods in respect to periods used for geothermal prospection (Babour and Mossier, 1980, Tezkan, 1994). Others account for the scale of induction space at defined period ranges and its implication on interpretation in this area (Menvielle and Tarits, 1986). The

investigated period range of this study is considered to be even sensitive to the local graben shape. Besides effects based on resistivity changes, magnetotellurics is also suitable to detect changes in strike, which may provide more insights to the stress distribution at depth.

The aim of the present study was to analyze the potential of 2D magnetotellurics and gravity for detection of geothermal resources in the Upper Rhine graben in general. Since the Soultz site is the most well-known and investigated site, a first E-W trending profile of an approximate length of 12 km has been chosen across the Soultz horst approximately on the latitude of the well end of GPK4 for magnetotelluric studies. The analysis of gravity has been performed on the existing database of the Leibniz Institute for Applied Geosciences (LIAG, Hannover) and the BRGM (Orleans).

2. ANALYSIS OF GRAVITY DATA

Different gravity data in the area of Xmin: 375000 km, Xmax: 500000 km, Ymin: 5385000 km, Ymax: 5485000 km (WGS 84/UTM Zone 32N) have been used for the following analyses: 1) the data summarized in the FIS Geophysik of the LIAG including data from Geophysikalische Reichaufnahme (1943-45, 695 measuring points), Wintershall (1952-53, 72), Rv. Saarland (1960, 1), Pfälzer Wald (1961, 153), Baden-Baden (261), Pfälzer Wald II (1986-99), Oberrheintal (1987, 42) and 2) data summarized at Bureau Gravimétrique International: "Carte gravimétrique de la France au 1/200000" and "Carte gravimétrique de la France au 1/80000". All data are reduced with a density of 2670 kg cm^{-3}. In order to avoid boundary effects in the forward modeling and inversion data evaluation has been carried out on a by about 4 x 4 times larger area than the later area of investigation. In order to obtain a regular distribution the Bouguer data were interpolated using the gravity maps on a 200 x 200 m grid. The constant offset of 7.7 mgal between the French and German data were corrected by adding this value to the French data. The well known MOHO anomaly in the Upper Rhine valley (Wenzel *et al.*, 1991) was estimated and subtracted from the Bouguer data by a Butterworth filter with a wave length of 70 km using Oasis Montaj (Geosoft in cooperation with TerraSys, Hamburg, Germany). The residual Bouguer anomalies (Figure 1) were used for forward modeling and inversion in the 3D Geomodeller (Intrepid).

The basis of the forward modeling and inversion is a geological 3-D model (Figure 2) including the major geothermally relevant faults and formation such as the Main Boundary Fault, Kutzenhausen- and Soultz-Faults and the Reimerswiler Fault, the Muschelkalk, Buntsandstein and the granitic basement, as well as the Tertiary, Jurassic and Keuper (Schill *et al.*, 2009). The following procedure has been applied for analyzing the gravity data: 1) forward modeling of the regional geological modeling, 2) inversion of the residual Bouguer data, 3) 2nd forward modeling of a geological model modified according to the results of the inversion.
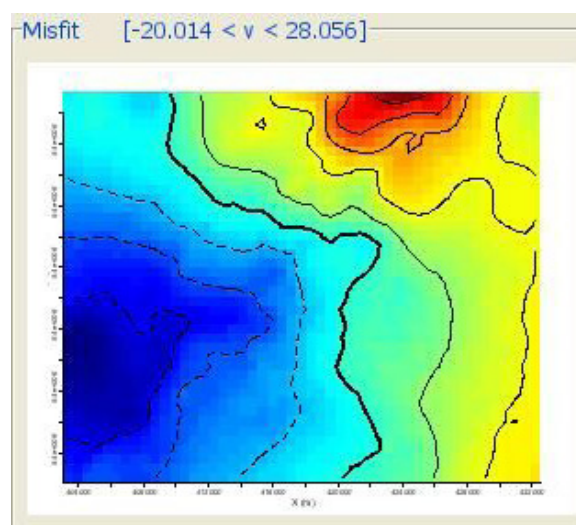
2.1 Forward Modeling of Bouguer Anomaly from a Geological 3D Model

The results of forward modeling the Bouguer anomaly (Figure 3) on the basis of the geological 3D model (Figure 2) reveal a large misfit between -20 and 28 mgal (Figure 4) when comparing to the residual Bouguer anomaly, which varies between about -20 and 25 mgal in the investigation area of Soultz-sous-Forêts (Figure 1).

The differences in gravity resulting from forward modeling are dominated by the density differences between the Mesozoic sedimentary Voges and the Pfälzer Wald in the NW and the younger sedimentary basin in the SE. Different starting densities for the formations do not lead to significant improvement of the misfit. In the following an inversion of the residual Bouguer anomaly has been performed in order to investigate the reason for this strong misfit.
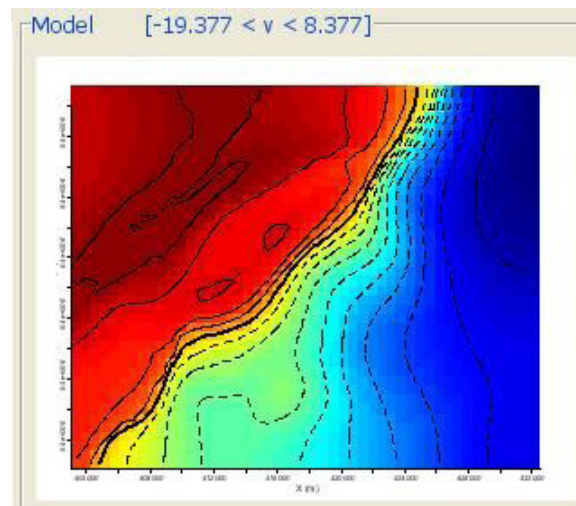
Figure 3: Results of the forward modeling of the Bouguer anomaly from the geological 3D model (Figure 2) of the geothermal area of Soultz-sous-Forêts (v: Bouguer anomaly in mgal).

Figure 4: Misfit between the forward modeled Bouguer anomaly from the geological 3D model (Figure 2) of the geothermal area of Soultz-sous-Forêts (v: misfit of the Bouguer anomaly in mgal) and the residual Bouguer anomaly (Figure 1).

2.2 Inversion of the Residual Bouguer Anomaly

The inversion of gravity has been carried out in the 3D Geomodeller (Intrepid) using a voxel discretization of the geological model in order to take into account the lithology. The geological unit for each voxel is initially assigned from the starting model. Density is then assigned according to the geological unit. Both can be variable during the inversion process. The inversion process is based on a Markov Chain Monte Carlo formulation, which is solely used to

accept/reject each candidate model, changing only one voxel at each iteration. The single voxel to be adjusted is selected randomly. The assigned geologic unit for the selected voxel may be changed to match that of an adjacent voxel on a random basis. The assignment of a density difference value is by random selection according to the probability function defined for the relevant geologic unit. The algorithm explores a wide range of possible models, all of which have a computed response which have a known likelihood based on how well it matches the observed data; thus, potentially many millions of possible models are examined, and the inversion results are presented in terms of the probabilities (Guillen *et al.*, 2004).

Variable geological units and density resulted in unrealistic geological models, where the Mesozoic sediments disappeared from the model. Therefore, in the presented inversion procedure only density variation was allowed. The results of inversion generally reveal an error of ±0. The larger deviation from the observed residual Bouguer anomaly in the area of the Main Boundary Fault of about 4-7 mgal are attributed to large variability in density. The units at the graben shoulders incorporate leucogranites (2550-2600 kg m^{-3}), monozonitic granites and granodiorites (2600-2650 kg m^{-3}) and gneisses and metavolcanics (2650-2850 kg m^{-3}) (Rotstein *et al.*, 2006).

The inversion result shown in Figure 5 represents the mean density of the wide range of possible inversion models along an E-W profile across the geothermal reservoir of Soultz-sous-Forêts. It reveals significant density anomalies in the basement. Mainly basement underneath the horst of Soultz-sous-Forêts is characterized by a comparatively low mean density of about 2500 kg m^{-3}. This may be attributed to leucogranitic bodies in this structure, supported by geological observations in the wells EPS1 and GPK1 (Genter *et al.*, 1995). An alternative explanation is a strong fracturation in the horst structure.

A second major structure of relatively higher density has been identified in the North of the investigation area, which corresponds to the maximum gravity anomaly of up to 25 mgal (Figure 1) in the residual Bouguer anomaly.

2.3 Second Forward Modeling of Bouguer Anomaly Including the Results of Inversion

For the second forward modeling the geological was modified according to the findings in the inversion. The basement was subdivided into three different types: 1) normal granitic basement, 2) low-density basement

underneath the horst of Soultz-sous-Forêts, and 3) a high-density body in the North of the investigation area (Figure 6). The geometry of the different bodies was estimated from the 3D inversion.

The result of the second forward modeling was a reduction of the misfit by half to v=-12 to 16 mgal.

3. ANALYSIS OF MAGNETOTELLURIC DATA

A number of 16 sites have been investigated on an E-W profile of approximately 12 km length across the horst structure at the latitude of the geothermal site of Soutlz-sous-Forêts extending about 6 km to the East and West (Geiermann and Schill, subm.). The site spacing is 0.8 km in average and varies between 0.5 and 2 km. Measurements have been accomplished using the multichannel geophysical measurement system GMS-06 (Metronix Inc.) including three broadband induction coil magnetometers MFS-06 (10000 Hz to 0.001 Hz) and four non-polarizable PbPbCl-electrodes distributed at a distance of 100 m in N-S and E-W direction. The ADU-06 logger and magnetometers are located in the centre, whereas the three induction coils are oriented N-S, E-W and vertical at a distance of 10 m to the data logger and at least 1 m to electric field wires. Three frequency bands have been measured at each site: The HF band (sample frequency 40960 Hz, frequency range 500-20000 Hz) runs 7 s by default; for the LF1 band (sample frequency 4096 Hz, frequency range DC-1000 Hz) a recording time of 15 min and for the LF2 (sample frequency 64 Hz, frequency range DC-30 Hz) band of two days has been chosen. A number of 7 stations have been operated contemporaneously with a remote reference station at Vogelsberg (Germany) registering the magnetic field variation in N, E, and vertical direction. The distance between the Vogelsberg and the area of investigation is of approximately 200 km.

3.1 Processing of Magnetotelluric Data

A coherency analysis was conducted to investigate the potential of remote reference processing. Further, data processing includes filtering and re-sampling of the time series and a notch filter to eliminate the influences of the 16 2/3 Hz railway power supply. Finally the estimation of the impedance tensor from the spectra was done by statistical means. We used and compared two independent processing softwares (Geiermann and Schill, subm.), Mapros (Metronix Inc.) and WinGLink (Geosystems). Both allow for remote referencing to reduce the influence of uncorrelated noise.
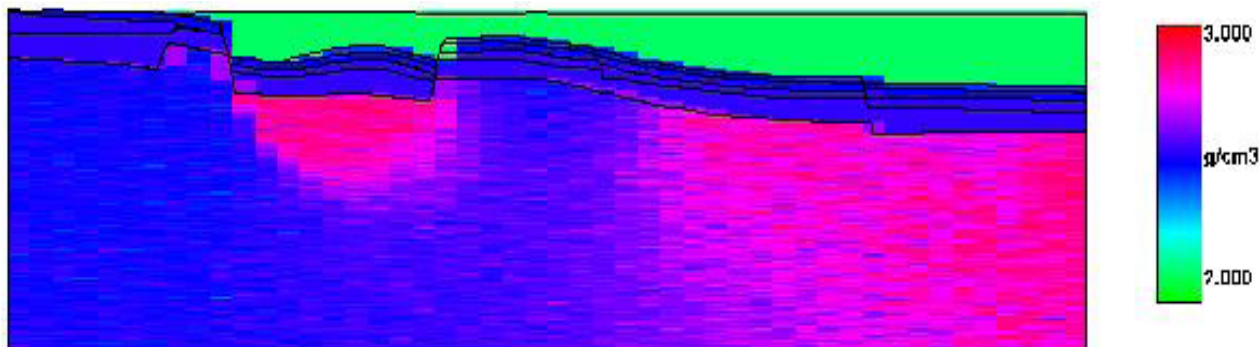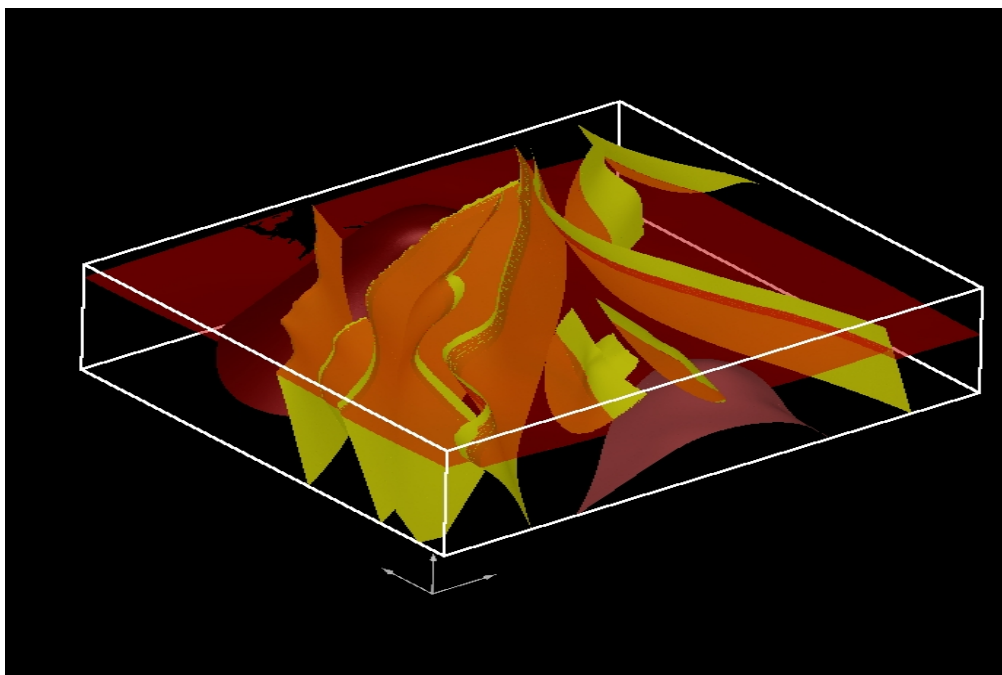

Figure 5: Mean density distribution resulting from inversion of gravity data for a representative E-W profile across the geothermal reservoir of Soultz-sous-Forêts. (E-W extension 29 km, altitude a.s.l.: -8000 to 250 m). Black lines represent the geological starting model.

Figure 6: Geometry of the granitic basement (transparent) and the two additional bodies in the basement (dark red: body with relatively higher density, light red: body with relatively smaller density).

The first processing with Mapros has been carried out for all frequencies, while the second processing with WinGLink (Geosystem) was limited to the LF2 band since information on the target depth is contained in this band and processing of the whole spectrum revealed no significant improvement in quality of the transfer functions compared to Mapros processing. WingLink processing applies cascade decimation (Wight and Bostick, 1980) to compute power spectra. At each level windows of 32 points are cosine tapered (von Hann-Window) and transformed into frequency domain by computing the 6th and 8th Discrete Fourier Transform (DFT). The estimation of transfer functions is carried out using a modified jack-knife method (Jones and Jödicke, 1984). Each site has been processed by maximizing coherency. Single site processing results could be improved by applying maximization of the multiple coherencies between one of the outputs and both inputs. Generally, remote referencing yields best results. A cross-power editor was used for manual rejection of elements from final stacking, in particular for the period range of 1 to 10 s. This was a crucial step in data improvement and resulted in more consistent apparent resistivity curve with respect to the phase curve.

After processing with Mapros (Figure 7), three distinct period ranges can be distinguished among all sites. Here exemplarily Site EMM is given, where the data is unrotated. In the first one, from $1.25 \cdot 10^{-4}$ to 0.05 s, apparent resistivity varies between a few hundred Ωm at short periods and 1 Ωm at 0.05 s. The phase angle decreases from 90 to 60° in this range. This peculiar behavior could be related to a special processing setting in Mapros and was avoided in the further proceeding. The second period range reveals smooth and consistent values in the apparent resistivity and in the phase between 0.05 and 1 s. The apparent resistivity decreases linearly from some tens to 1 Ωm and the phase angle varies between 60° and 45°. The last range covers the longest periods. Between 1 and 10 s the curves reveal steep slopes and scatter, related to the MT- dead band. Around 100 s most sites reveal consistent

apparent resistivity and phase and the XY– and YX-polarizations reveal clearly different behavior. The apparent resistivity shows differences of one to two decades. In the following, we call this feature splitting. Splitting could not be attributed to strong bias but interpreted as sign of higher dimensional inductive effects, if occurring in both apparent resistivity and phase. The large errors at longest periods are attributed to relatively short recording times. This goes along with a strongly scattered phase, in particular of the YX-component. In summary, the curves are seriously biased and scattered over a wide range of periods and Hilbert transformation could not be applied successfully. In particular, at frequencies from 1 to 1000 s, corresponding to the target depth, transfer functions could not be analyzed in terms of dimensionality nor interpreted otherwise.
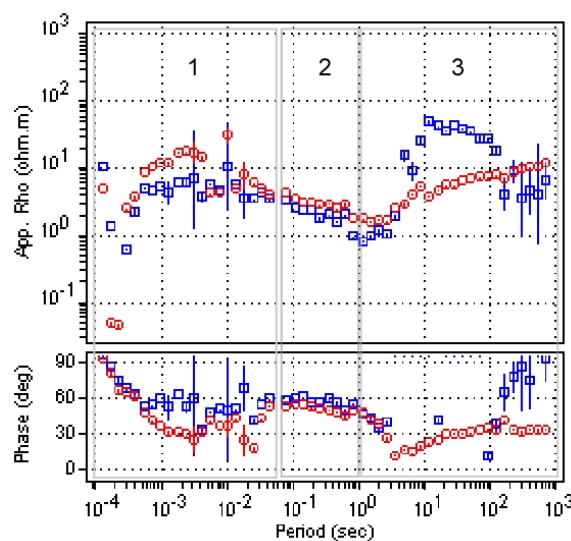
Figure 7: Transfer functions of site EMM after Mapros processing (unrotated).
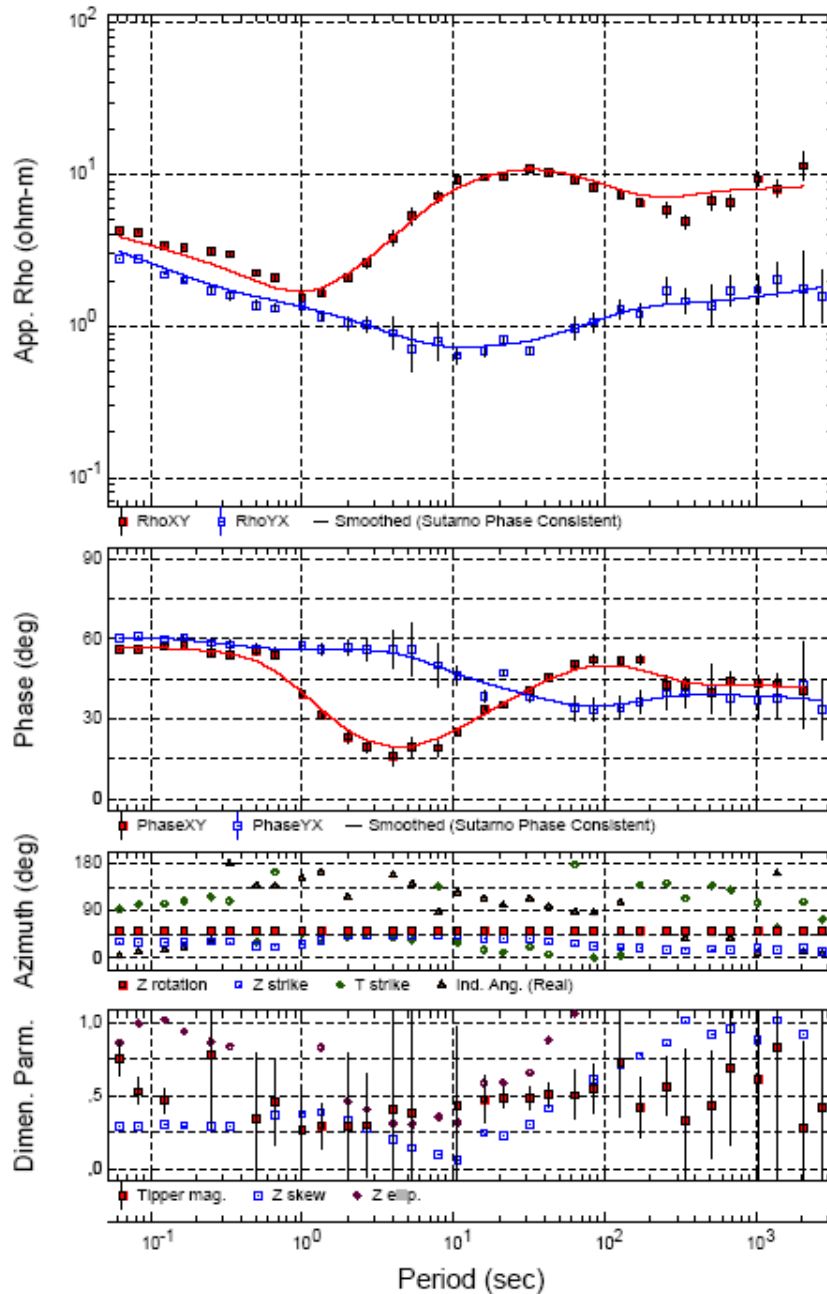
Figure 8: Apparent resistivity, phase angle, swift angle (Z strike), and skew (Z skew) of the representative site EMM reprocessed and rotated to 52° including "Sutarno Phase Consistent Smoothing" for the apparent resistivity and phase.

A result of the reprocessed LF2 band using remote reference and WinGLink processing is presented in Figure 8 (already rotated to 52°). For all sites except one, the scatter of the phase could be reduced significantly. Thus smooth curves with phase angles decreasing from 60° at about 0.06s to 15° at a few tens of seconds are obtained. It reveals splitting already at 1 s with a decrease in phase of the XY-component to a 15°. In a few cases in the MT-dead band also angles close to 0° are observed and attributed to bias. Among the sites the XY-component appears to be better estimated than the YX-component, in particular at periods longer than 200s. The bias in the apparent resistivity could be reduced applying processing with remote reference and manual selection of elements to stack. The apparent resistivity is about 3 to 7 Ωm at 0.06 s and decreases to about 1 Ωm at a few tens of seconds. Only at sites exhibiting strong bias, for which remote reference is not available, it decreases to <1 Ωm. A splitting of the

apparent resistivity for XY- and YX-components is consistent with the phase splitting. For long periods, values in the XY-component are <12 Ωm and >1 Ωm in the YX. In summary, remote reference processing leads to significant improvement in both, phase angle and apparent resistivity for all sites except one. One site reveals consistent results without remote referencing. The overall improvement in the phase angle and apparent resistivity for biased or scattered period ranges allows for interpretation in terms of dimensionality and eventually static shift.

At short periods to a few seconds the phase angle and apparent resistivity are congruent and rotationally invariant for the XY- and YX-components with a small offset, indicating a small static shift. Except from one site, at short periods the swift skew is generally 0 to <0.2. At the site closest to the graben boundary nearly constant skew of about 0.3 and small offset between the phases of the XY-

and YX-components are observed, perhaps indicating a near-surface 3D effect. However, in general it can be assumed that, in the short period range a 1-D environment is mapped by the sounding. In the period range between a few to tens of seconds, the onset of the splitting in phase angle and apparent resistivity, which is most prominent at a rotation angle of 52°, is observed. Close to the boundary of the graben it occurs at 3 s. It is shifted to longer periods along the profile towards the East. From periods larger than 10 s, the skew starts to increase slightly to about >0.25 at 40 s. In summary, the maximization of the splitting at rotation of 52° indicates a 2-D environment with a 52° strike direction, which is also indicated by calculation of Swifts angle. The angle of 52° corresponds to the local border shape of the graben structure. Thus, we have defined TE and TM mode from the XY- and YX-component. Increasing diagonal elements and the increasing trend in skew for periods larger than 40s is an indication for increasing influences of 3-D effects.

Dimensional analysis reveals transition from 1-D to 2-D to 3-D subsurface structures with increasing period. The dominant feature is the 2-D response indicated by splitting between 1 and 10 s attributed to the local graben border striking N52°E (local scale). At larger periods presumably the regional N20°-30°E strike of the Rhine Graben dominates (regional scale). 2-D inversion is therefore only constrained by the period range up to 40 s.

3.2 2-D Inversion of Magnetotelluric Data

The inversion algorithm (Rodi and Mackie, 2001) computes solutions to the inverse problem by minimizing an objective function ψ. The solutions are regularized by incorporating smoothness constrain in ψ. This accounts for the smoothness of a magnetotelluric sounding and its insensitiveness to sharp, small scale contrasts, instead favoring least-structure models. The regularization is implemented by defining the objective function (Tikhonov and Arsenin, 1977).

The inversion was carried out using the 10 sites projected on a profile at N142°E (Geiermann and Schill, subm.). The total mesh dimension is of about 240 x 120 km horizontal and depth. The profile extends to about 8 km length in this projection. The mesh extension and meshing of the profile area follows the rules preventing the algorithm from numerical instabilities (Rodi and Mackie, 2001). The active mesh area was limited vertically to approximately one skin depth of the lowest period and horizontally to an adjustment length of approximately three skin depths. The 2-D inversion algorithm was applied using Sutarno phase consistent smoothed data after having masked outliners and rotation by 52°. A regional a priori model accounting for the geometry of the Rhine graben has been used. In the inversion procedure regularization was switched to smoothest variation away from starting model. TE and TM mode as well as phase and apparent resistivity have been inverted simultaneously with 100 iterations. The error floors were initially set to 25%, then first the phase error floor was reduced to force fitting of the model to the phase angle (final values: 5%). The trade-off parameter was reduced stepwise to allow for modeling of structures with relatively small scale (final value: $\tau=1$). The approximate depth and thickness of the known Couche rouge structure was labeled as tear zone to omit smoothing-out of this thin, but electrically prominent structure.
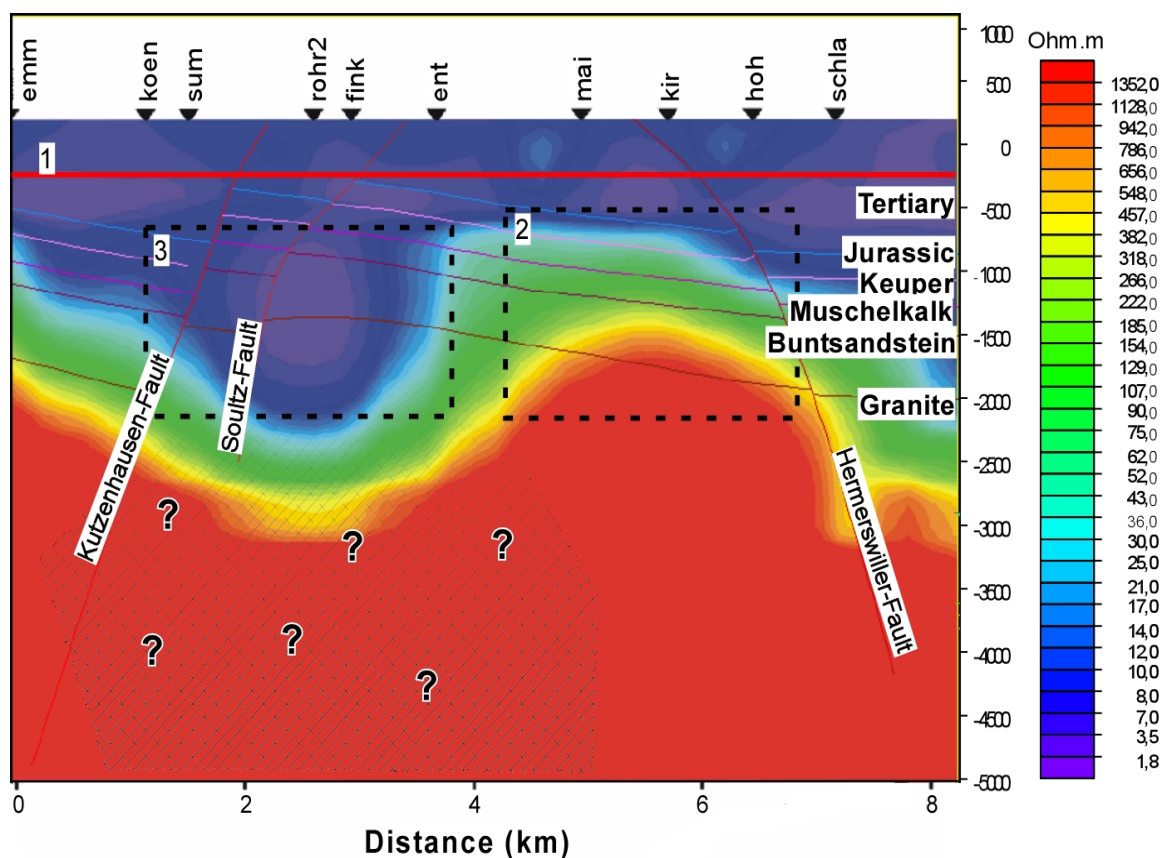

Figure 9: Interpreted section of 2D inversion of Sutarno phases consistent smoothed data on profile N142°E (rms = 2.28). Gridding of the inversion result was performed using spline interpolation. Superimposed are the major faults and formation boundaries of a 3D geologic model (Schill et al., 2009).

The result of the inversion is presented in Figure 9. The over-all rms error is 2.28 and the individual site-rms is always below 3. Generally, the Rheingraben model is well represented. During all inversion steps the boundary between the conducting half layers with resistivities $< 10\,\Omega$m at depth down to about 750 m and the resistive underlying space with resistivities of $> 1350\,\Omega$m was preserved. A conductive zone between site SUM and site ENT, however, extends vertically to more than 2000 m. The conductive feature below about 200 m can be attributed to the clay-rich Couche Rouge (red line). A thickness of 50m to 100m would correspond to the thickness of the Couge rouge (Cautru, 1987).

Box-2 shows a part of the profile, which is in good agreement with the a priori model. The Triassic sediments coincide with an area of increasing resistivity from some tens to a few hundred Ωm. The top of basement is marked by a strong increase in resistivity to more than 1000 Ωm.

The layering is disturbed by a conductive anomaly (see Box-3). Its center with average resistivity of 3 Ωm extends over the Buntsandstein formation into the granitic basement. It coincides partly with the Soultz- and Kutzenhausen-Fault. These low resistivities in especially in the granitic basement indicate a relatively high degree (still below 1 % of total rock volume) of interconnected pore-space (Geiermann and Schill, subm.). Deeper lying structures could not be resolved in 2-D inversion, since 3-D features are indicated at periods >40 s.

4. DISCUSSION AND CONCLUSION

Generally both geophysical methods reveal a significant good reproduction of the major structures of the Upper Rhine valley. In the inversion of gravity data on the basis of the regional geological 3D model, the Tertiary graben fills and Mesozoic sediments reveal the mean densities of about 2000 kg m^{-3} and 2500 kg m^{-3} (Figure 5). These densities are lower compared to earlier studies (Mesozoic sediments: 2650–2700 kg m^{-3} in the shoulders and 2550–2600 kg m^{-3} in the graben; Tertiary sediments: 2350–2450 kg m^{-3}) (Rotstein *et al.*, 2006) and differences for the Mesozoic sediments in the shoulder and the graben, however, were not resolved. The mean density of the basement can be variable as observed in the basement rocks outcropping on the graben shoulder (Rotstein *et al.*, 2006). Our inversion results in major density differences in the basement. It reveals a difference between the basements below the shoulders with a mean density around 2500 kg m^{-3} and below the graben with mean densities up to 3000 kg m^{-3} (Figure 5). The basement underneath the horst of Soultz-sous-Forêts is characterized by a comparatively low mean density of about 2500 kg m^{-3} indicating either leucogranitic bodies in this structure, supported by geological observations in the wells EPS1 and GPK1 (Genter *et al.*, 1995) or a strong fracturation.

Elevated porosity and fracture density are found in major fracture zones, extending laterally on metric scale and longitudinally on metric to hecto-metric scale (Genter, 1989) and they are considered to be interconnected (Dezayes and Genter, 2008). In order to derive bulk resistivity on hector-metric to kilometric scale, resolved by magnetotellurics at relevant depth, a conceptual resistivity model based on Archie's Law (Archie, 1942) and average porosity was set up for the granitic basement. The bulk resistivity ρ_b is calculated using a parallel connection of four possible rock facies (Equation 1).

$$\rho_b = \rho_f \cdot F_g = \rho_f \frac{1}{\left(\Phi_r F_r^{-1} + \Phi_d F_d^{-1} + \Phi_{mf} F_{mf}^{-1} + \Phi_p F_p^{-1} \right)} \quad (1)$$

where F_i is the respective formation factor with a fluid saturation S = 1 and ρ_f is the resistivity of the fluid.
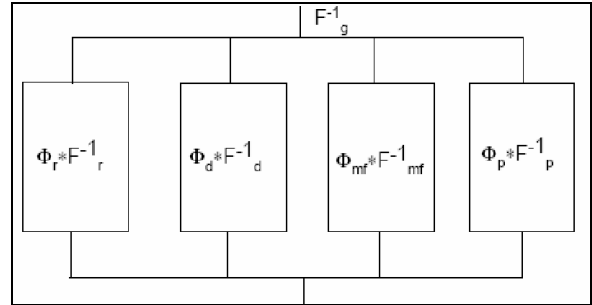
Figure 10: Sketch of parallel connection of four facies with different properties composing an equivalent bulk factor formation.

The volume fractions $\Phi_{r, d, mf, p}$ of the three alteration facies are varied from 0% to max% in 0.5% steps for different stages of total alteration (max = 5, 10, 20). The four different rock facies are characterized by different formation factors comprised of typical values for porosity φ, cementation factor m and geometric factor a. Porosity values are taken from the Soultz granite (Genter *et al.*, 1998). It should be mentioned that the "direct connection facies" corresponds to a formation factor of 1. The electrically conducting phase is brine with a salinity of 100 g l^{-1} and a temperature of about 130 °C (at the boundary between the Buntsandstein and granitic basement). According to our model, to an alteration stage of 20 % of total rock mass (upper limit of total alteration stage in this parameter setting) at least 1% is represented by "direct connection facies" in order to obtain bulk resistivites below 2 Ωm. These well conducting pathways can be distributed irregularly over the rock volume which is covered by the anomaly. Those small scale heterogeneities are not resolved by the magnetotelluric method which rather gives a volumetric average. Borehole logging, in turn, is very sensitive to changes in the physical properties on a small scale, but samples a much smaller volume. This difference in resolution may be an explanation for the differences in the order of one to two magnitudes between the results from logging and from magnetotelluric measurements.

The comparison between gravity and magnetotelluric data shows that the regional gravity inversion was able to detect a density anomaly of the horst structure, which can be related to either the occurrence of leucograntites or strong fracturation in the deeper part of the granitic basement. The 2-D magnetotelluric inversion could be used in order to investigate the upper part of the horst structure more in detail. The ongoing study of 3-D magnetotelluric measurements and refinement of the gravity inversion are expected to provide the possibility of joint interpretation of the two methods over the entire horst structure.

ACKNOWLEDGEMENTS

geothermal site. The Soultz team in particular N. Cuenot and G. Krall were always available for help during the field work. The field work was greatly supported by M. Ernest Franck. We would also like to thank M. Krüger from TerraSys for the excellent and interesting collaboration. The comments of the reviewer help to improve significantly the quality of the paper.

REFERENCES

Albouy, Y. & Fabriol, H., 1981. Telluric measurements and differential geomagnetic soundings in the Rhinegraben (period range 1-125s), *Geophysical Journal of Royal Astronomic Society,* 65**,** 91-101.

Aquilina, L., Dreuzy, J.-R.d., Bour, O. & Davy, P., 2003. Porosity and fluid in the upper continental crust (2 to 4 km) inferred from injection tests at the Soultz-sous-Forets geothermal site, *Geochimica et Cosmochimica Acta,* 68**,** 2405-2415.

Archie, G.E., 1942. The electrical resistivity log as an aid in determining some reservoir characteristics, *T. Am. I. Min. Met. Eng.,* 146**,** 54-62.

Babour, K. & Mossier, J., 1980. Direct determination of the characteristics of the currents responsible for the geomagnetic anomaly of the Rhinegraben, *Geophysical Journal of the Royal Astronomic Society* 65**,** 327-331.

Bächler, D., 2003. Coupled Thermal-Hydraulic-Chemical Modelling at the Soultz-sous-Forêts HDR reservoir (France), PhD Thesis, ETH Zurich, Zurich.

Cautru, J.P., 1987. Coupe géologique passant par le forage GPK1 calée sur la sismique réflexionBRGM, Orleans.

Dezayes, C. & Genter, A., 2008. Large-scale fracture zone network based on Soultz borehole data. *in EHDRA Scientic Conference*, ed Genter, A., Soultz-sous-Forêts.

Edel, J.-B., Schulmann, K. & Rotstein, Y., 2007. The Variscan tectonic inheritance of the Upper Rhine Graben: evidence of reactivations in the Lias, Late Eocene–Oligocene up to the recent

International Journal of Earth Sciences (Geologische Rundschau), 96**,** 305-325.

Geiermann, J. & Schill, E., subm. 2-D Magnetotellurics at the geothermal site at Soultz-sous-Forêts: Resistivity distribution to about 3000 m depth, *Geosciences*.

Genter, A., 1989. Geothermie Roches Chaudes Seches: le granite de Soultz-sous-Forets (Bas Rhine, france). Fracturation naturelle, alteration hydrothermale et interaction eau-roche, Universite de Orleans, Orlean.

Genter, A., Dezayes, C., Gentier, S., Ledesert, B. & Saussé, J., 1998. Conceptual Fracture Model at Soultz Based on Geological Data. *in 4th Int. HDR Forum*, Strasbourg.

Genter, A., Traineau, H., Deszayes, C., Elsass, P., Ledesert, B., Meunier, A. & Villemin, T., 1995. Fracture analysis and reservoir chracterization of the granitic basement in the HDR Soultz Project (France), *Geothermal Science and Technology,* 4**,** 189-214.

Guillen, A., Courrioux, G., Ph.Calcagno, Lane, R., Lees, T. & McInerney, P., 2004. Constrained gravity 3D litho-inversion applied to Broken Hill. *in ASEG 2004 - 17th Geophysical Conference* CSIRO, Australia.

Gutscher, M.-A., 1995. Crustal structure and dynamics in the Rhine Graben and the Alpine foreland, *Geophysical Journal International,* 122**,** 617-636.

Hurter, S. & Schellschmidt, R., 2003. Atlas of geothermal resources in Europe, *Geothermics,* 32**,** 779-787.

Jones, A.G. & Jödicke, H., 1984. Magnetotelluric transfer function estimation improvements by a coherence-based rejection technique. *in 54th Annual International Meeting*, ed Geophysics, S. o. E., Atlanta (Georgia).

Kohl, T., Bächler, D. & Rybach, L., 2000. Steps towards a comprehensive thermo-hydraulic analysis of the HDR test site Soultz-sous-Forêts. *in World Geothermal Congress 2000*, pp. 2671-2676, ed Iglesias, E., Blackwell, D. Hunt, T., Lund, J., Tamanyu, S., Kimbara, K., Kyushu - Tohoku, Japan.

Marquis, G. & Gilbert, 2002. Magnetotelluric measurements at GPK 1, pp. 4EHDRA, Soultz.

Menvielle, M. & Tarits, P., 1986. 2-D and 3-D interpretation of conductivity anomalies: example of the Rhine graben conductivity anomaly, *Geophysical Journal of the Royal Astronomic Society,* 86**,** 213-226.

Pauwels, H., Fouillac, C. & Criaud, A., 1992. Water-rock interactions during experiments within the geothermal Hot Dry Rock borehole GPKI, Soultz-sous-For~ts, Alsace, France, *Applied Geochemistry,* 7**,** 243-255.

Rodi, W. & Mackie, R.L., 2001. Nonlinear conjugate gradient algorithm for 2Dmagnetotelluric inversion, *Geophysics,* 66.

Rotstein, Y., Edel, J.-B., Gabriel, G., Boulanger, D., Schaming, M. & Muschy, M., 2006. Insight into the structure of the Upper Rhine Graben and its basement from a new compilation of Bouguer Gravity, *Tectonophysics,* 425**,** 55-70.

Schellschmidt, R. & Clauser, C., 1996. The thermal regime of the Upper Rhine Graben and the anomaly at Soultz, *Z. Angew. Geol.,* vol. 42**,** pp.40-44.

Schill, E., Kohl, T., Baujard, C. & Wellmann, J.F., 2009. Geothermische Ressourcen in Rheinland-Pfalz: Bereiche Süd- und Vorderpfalz, pp. 55Ministerium für Umwelt Forsten und Verbraucherschutz, Mainz.

Simpson, F. & Bahr, K., 2005. *Practical Magnetotellurics,* edn, Vol., pp. Pages, Cambridge University Press, Cambridge.

Spichak, V., Zakharova, O. & Rybin, A., 2007. Estimation of the sub-surface temperature by means of magnetotelluric sounding

in Thirty-Second Workshop on Geothermal Reservoir Engineering Stanford University, pp. SGP-TR-183, Stanford, California.

Telford, W.M., Geldart, L.P. & Sheriff, R.E., 1990. *Applied Geophysics,* Second Edition edn, Vol., pp. Pages, Cambridge University Press, Cambridge.

Teufel, U., 1986. Die Verteilung der elektrischen Leitfähigkeiten in der Erdkruste unter dem Schwarzwald, ein Beispiel für Möglickeiten und Grenzen der Interpretation von Audiomagnetotellurik, Magnetotellurik, Erdmagnetischer Tiefensondierung, PhD, Ludwig-Maximilian Universität, München.

Tezkan, B., 1994. On the detectabilityof highly conductive layer in the upper mantle beneath the Black Forest

crystalline using magnetotelluric methods, *Geophysical Journal International,* 118**,** 185-200.

Tikhonov, N. & Arsenin, V.Y., 1977. *Solutions of Ill-Posed Problems,* edn, Vol., pp. Pages, Winston & Sons, Washington, D.C.

Wenzel, F., Brun, J.-P. & group, E.-D.w., 1991. A deep reflection seismic line across the Northern Rhine Graben, *Earth and Planetary Sciences,* 104**,** 140-150.

Wight, D.E. & Bostick, F.X., 1980. Cascade decimation - A technique for real time estimation of power spectra. *in IEEE international Conference on ICASSP'80,* pp. 626-629.